European Journal of Agronomy 106 (2019) 1–11

Contents lists available at ScienceDirect

European Journal of Agronomy

journal homepage: www.elsevier.com/locate/eja

The impact of climate change on barley yield in the Mediterranean basin

Davide Cammarano[a,*], Salvatore Ceccarelli[b], Stefania Grando[c], Ignacio Romagosa[d], Abdelkader Benbelkacem[e], Tanek Akar[f], Adnan Al-Yassin[g], Nicola Pecchioni[h,i], Enrico Francia[i], Domenico Ronga[a,i,j]

[a] James Hutton Institute, Invergowrie, DD25DA, Scotland, UK
[b] Rete Semi Rurali, Italy
[c] International Consultant, Italy
[d] Agrotecnio Center, Universitat de Lleida, Spain
[e] INRAA, Algeria
[f] Akdeniz University Faculty of Agriculture, Dept. of Agronomy, Antalya, Turkey
[g] Consultant and barley breeder, National Agricultural Research Center, Amman, Jordan
[h] Council for Agricultural Research and Economics (CREA) Research Centre for Cereal and Industrial Crops (CREA-CI), S.S. 673 km 25,200, 71122 Foggia, Italy
[i] University of Modena and Reggio Emilia, Department of Life Sciences, Via G. Amendola 2, 42122 Reggio Emilia, Italy
[j] Council for Agricultural Research and Economics – Research Center for Animal Production and Aquaculture (CREA-ZA), Viale Piacenza, 29, 26900, Lodi, Italy

ARTICLE INFO

Keywords:
Barley
Mediterranean environment
Climate change
Soil water content
Drought
Heat
Climate extremes

ABSTRACT

Barley is an important cereal crop for the arid and semi-arid Mediterranean environments. Future climate projections show that Mediterranean countries will get drier and hotter. The objectives of the study are to: i) simulate the impacts of different climate projections and different sowing dates on yield; ii) quantify the importance of heat and drought on barley yield at different growth stages and sowing dates; iii) quantify the contributions of sources of uncertainty among inter-annual variability, adaptation options and climate projections. Nine locations across the Mediterranean basin were used to calibrate and evaluate the Decision Support System for Agrotechnology Transfer (DSSAT) model. At each location the 40 Global Circulation Model (GCM) outputs (RCP4.5, Mid of the Century) showed an increase in mean growing season temperature between 0.9 and 2.16 °C, while changes of growing season rainfall were between -24 and +24%. Therefore, at each location a drier (Dry), mid (Mid), and wetter (Wet) projection was selected. Overall, there was a 9% reduction in grain yield under climate change; but the mean yield change was -27%, +4%, +8%, for the Dry, Mid, and Wet scenarios, respectively. The results of the simulations under the Wet scenario showed a higher variability of yield response. There was an interaction between the soil type, the amount of rainfall, the extractable soil water content and the maximum air temperature. Because of these relationship water-stress during the vegetative stage was experienced, affecting expansive growth. At the same time, the high number of days with *Tmax* > 34 °C caused higher soil water depletion by the plant and therefore lower yields under the Wet scenario. The inter-annual weather variability impacts barley yield irrespective of the sowing dates and the future projected climate. In conclusion, the impact of future climate on barley yield in the Mediterranean is negative but some locations will be less affected than others.

1. Introduction

Barley is an important cereal crop for the arid and semi-arid Mediterranean environments. It is cultivated from the equator to the Arctic Circle and at different elevations (Ceccarelli et al., 2011; Dawson et al., 2015). Europe produces about 63% of the world's barley with most of it under rainfed conditions (FAOSTAT, 2018). Evidence suggests that cereals crop yield is peaking worldwide, and barley yields in Mediterranean countries follow the same trend (Martre et al., 2015; Dawson et al., 2015). Mediterranean environments are characterised by hot dry summers and humid, cool winters with high variability in patterns of rainfall and temperature impacting yield gains (Brisson et al., 2010).

Future projections of climate trends show that Mediterranean countries will get drier and hotter and might result in severe yield reduction (Semenov et al., 2014; Senapati et al., 2018). During

* Corresponding author.
E-mail address: davide.cammarano@hutton.ac.uk (D. Cammarano).

https://doi.org/10.1016/j.eja.2019.03.002
Received 15 November 2018; Received in revised form 10 February 2019; Accepted 11 March 2019
Available online 19 March 2019

reproductive development, both heat and drought have negative effects on final yield (Semenov et al., 2014; Asseng et al., 2015). However, both factors are part of the soil-plant-atmosphere system and they dynamically interact within such system. Mean air temperature is the main driver of canopy and leaf temperature, affecting photosynthetic rates, and higher temperatures will negatively influence yield by damaging reproductive organs and accelerating senescence rates (Asseng et al., 2011). Soil moisture limitation will have negative impacts on crop expansive growth and regulating leaves' stomatal conductance (Huntingford et al., 2005). When soil water contents and mean air temperature are not limiting both photosynthesis and transpiration at leaf's level will occur at normal rates (Saseendran et al., 2008). At higher air temperatures and low vapour pressure deficit (VPD) plants open the stomata to avoid heat stress, increasing the inter-cellular CO_2 concentration and biomass growth. When soil water content is the limiting factor the stomata are closed, causing dissection, negative impact on photosynthesis, low intercellular CO_2 concentration and therefore lower biomass (Kobza and Edwards, 1987). In addition, in Mediterranean environments, where crops rely on soil moisture stored prior sowing, an adequate level of soil available water content is vital to achieve certain yield levels. Therefore, the patterns of rainfall prior sowing will also be an important determinant of crop yield (Passioura, 2006).

To explore the impacts of climate variability and changes on grain production, crop simulation models (CM) are generally used. They simulate daily growth, development, and yield as influenced by daily weather, soil type, crop features and agronomic management (Cammarano and Tian, 2018). The rationale of using CM to explore the climate impacts is because they can extrapolate the daily interactions of soil water and nutrient beyond one single growing season (Jones et al., 2003). In addition to the use of CM, Global Climate Models (GCM) provide the atmospheric input of climate projections to such models.

A combination of data and modelling results have been used to explore the impact of environmental condition on crop production (O'Leary et al., 2015; Rötter et al., 2012). An ensemble of 30 wheat crop models was tested against field experimentations and at different locations worldwide, the application of such ensemble showed that global wheat production will fall by 6% for each °C of temperature increase (Asseng et al., 2015). Overall, on many crops important for food security (e.g. cereal, legumes, sugarcane) even a moderate increase in air temperature will likely have a major negative impact if no adaptation measures are taken. It is expected that negative impacts will be more relevant in developing countries (Rosenzweig et al., 2014; Lobell et al., 2008; Challinor et al., 2014; Porter et al., 2014). Therefore, adaptation options are the best option for maintaining future food needs. Challinor et al. (2014) and Porter et al. (2014) concluded that adaptation options could help to increase mean yield by about 7% regardless of the warming levels. In a recent study it was found that global barley yields will decline between 3–17%, depending on the geographical location, and in many areas of North Africa, the horn of Africa and South America (where it is an important food crop) the negative projected yield changes will impact food security (Grando and Gormez Macpherson, 2005; Xie et al., 2018).

Recent scientific efforts using CM focused on the effect of heat stress on development and yield (Asseng et al., 2016, 2015). Xie et al. (2018) studied the impacts of climate extremes on global barley yields, focusing on drought and heat stresses. However, there are, to the best of our knowledge, virtually no simulation studies on barley specific for the Mediterranean conditions where the impacts of projected changes of heat and drought on barley is explored; as well as the impact of agronomic adaptation options. Tao et al. (2018) developed a triple-ensemble probabilistic assessment by using a combination of CMs, model parameters, and climate projections to find the main source of uncertainty. The study did not focus on the impacts of climate change on barley per-se but helped to quantify that the major uncertainty was in the models' structure rather than the climate projections.

We hypothesize that, depending on the climate projection (e.g. drier or wetter), the impacts of changing agronomic practices might offset the negative impacts of climate change. In addition, the importance of future drought and heat stresses on barley yield will be explored prior sowing, at vegetative and reproductive stages. Finally, the sources of uncertainty coming from inter-annual climatic variability, adaptation strategy, and climate scenario were analysed. The objectives of the study are to: i) simulate the impacts of different climate projections and different sowing dates on yield; ii) quantify the importance of heat and drought on barley yield at different growth stages and prior sowing; iii) quantify the contributions of sources of uncertainty among inter-annual variability, adaptation options and climate projections.

2. Materials and methods

2.1. Study area

The study area comprises the Mediterranean basin; nine locations spanning from Northern Africa to Southern Europe were selected because data were available from a study of Francia et al. (2011), where several genotypes were tested in these locations for three years (2003, 2004, and 2005). No remarkable incidence of biotic stresses was

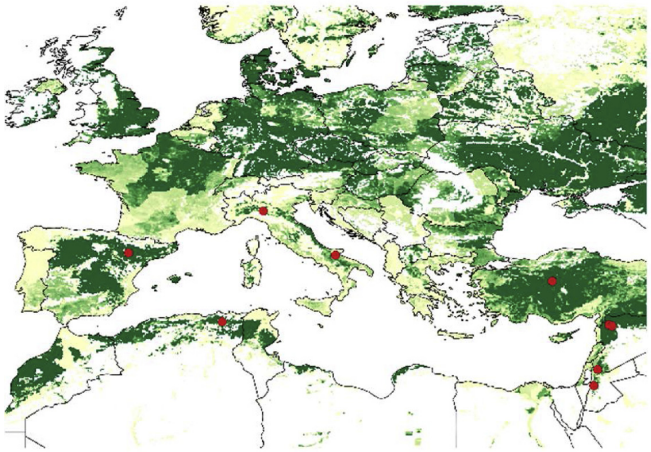

Fig. 1. The red dots indicate the locations of the study of Francia et al. (2011) used in the current work. The green area indicates the barley growing area and the intensity of the cultivation (For interpretation of the references to colour in this figure legend, the reader is referred to the web version of this article).

recorded at any site. During the three years, two locations had additional irrigation and all the others were rainfed. The geographical distribution of the locations is shown in Fig. 1. Information regarding the sowing, anthesis, maturity and yield were available in Francia et al. (2011). In addition, information on the soil water holding capacity were also available, and the co-authors of that study provided information regarding the soil texture and organic carbon levels.

2.2. Weather data

One growing season of daily weather data was available at each site. Daily values of solar radiation (MJ m^{-2} d^{-1}), maximum temperature (°C), minimum temperature (°C), and rainfall (mm) were used. To have a long-term weather data series, needed as baseline for our study, the daily data at each location were reconstructed for the period 1980–2010 using the NASA AgMERRA product (Ruane et al., 2015). Such dataset has been used in many climate change impact studies worldwide (Rosenzweig and Hillel, 2015; Elliott et al., 2015). To quantify the quality of the constructed time series the observed year of weather data was compared against the NASA AgMERRA.

2.3. Climate projections

The climate projections were obtained using the global Coupled Model Intercomparison Project Phase 5 (CMIP5) data for temperature, precipitation, and solar radiation (Taylor et al., 2012). To generate perturbed daily weather data, the DSSAT-Perturb software was used (ClimSystem, 2018). The software used the baseline weather data at each location, and by integrating the CMIP5 from 40 Global Circulation Models (GCM; Tab. A1), generates projected daily weather data. More details about algorithms behind the software are found in Yin et al. (2013). At each location, the future daily output of 40 GCMs were produced at a Representative Concentration Pathway 4.5 (RCP 4.5) Mid of the Century (Tab. A2). At each location, the percentage change in terms of growing season rainfall and temperature with respect to the baseline was calculated for each GCM. Then, a similar approach detailed in the study of Ruane and McDermid (2017) for each location was chosen to pick 3 site-specific GCMs. But, to narrow down the number of GCMs chosen, at each location three GCMs were selected. They were selected to provide similar amount of growing season temperature increase but "drier", "little" and "wetter" changes of rainfall with respect to the baseline.

2.4. Crop simulation

The DSSAT v4.7 was used for this study (Decision Support System for Agrotechnology Transfer), the CERES-Barley model was the crop-specific used (Jones et al., 2003; Hoogenboom et al., 2010). The input data for the model were the ones obtained at each experimental site, and a generic barley cultivar was calibrated (Tab. A3) using the observations reported in Table 1 in the study of Francia et al. (2011). The initial soil water and nitrogen content, known as "initial conditions", are two important parameters determining the quality of the simulation runs. In this study, the date of the initial conditions (when the crop model started running) were assumed to be after the generic harvest date for each location. Therefore, this allowed to start with a relatively dry soil profile (10% above the soil Lower Limit), while for the initial nitrogen in the soil experts' opinion from agronomists from each site were used. The nitrogen fertilizer management was also derived from experts' opinion and from local researchers at each location. The crop model was calibrated using the two irrigated sites and evaluated on the remaining sites.

The sowing dates used for the simulations ranged from mid-September to mid-January (sowing happening every 15 days; S1 to S8) at each location and were run for the baseline and for each of the 3 scenarios. The atmospheric CO_2 concentration used by the model for the baseline runs (1980–2010) was 360 ppm while at RCP4.5 it was 499 ppm. The model's runs were set up to re-initialize every growing season. Every growing season the models started with the same initial conditions, same sowing date, and same fertilizer management. The only thing that changed was the weather conditions. In this way, the impacts of climate and weather variability can be quantified.

Table 1
Results of the calibration and evaluation of the generic barley cultivar at three irrigated location for calibration and for the remaining locations for the evaluation.

Step	Variable	r^2	RMSE	d-Index
Calibration	*Heading*	0.99	4 *d*	0.99
	Maturity	0.96	9 *d*	0.98
	Yield	0.85	587 kg *DM* ha^{-1}	0.60
Evaluation	*Heading*	0.97	6 *d*	0.99
	Maturity	0.82	10 *d*	0.99
	Yield	0.55	1200 *kg DM* ha^{-1}	0.80

2.5. Statistical analysis

The goodness of fit of the simulated vs. observed data for calibration and evaluation was calculated using the Root Mean Square Error (RMSE) as follows:

$$RMSE = \sqrt{\frac{1}{n}\sum_{i=1} (y_i - \hat{y}_i)^2} \quad (1)$$

where y_i are the observations, $\hat{y}_i$ the simulations, and n is the number of comparisons. In addition, the Wilmott index of agreement (D-Index) was calculated (Wilmott, 1982). The index ranges from 0 (poor model) to 1 (good model). The index is a descriptive measure and can be widely applied to make cross-comparison between models (Wilmott, 1982). It is calculated as follows:

$$d - Index = 1 - \frac{\sum_{i=1}^{n} (y_i - \hat{y}_i)^2}{\sum_{i=1}^{n} (|y_i - \bar{y}| + |\hat{y}_i - \bar{y}|)^2} \quad (2)$$

Were $\bar{y}$ is the mean of the observed values. The relative grain yield change was calculated as:

$$RY = \frac{y_{future,\,k,\,i} - y_{baseline,i}}{y_{baseline,i}} * 100 \quad (3)$$

where $y_{future,\,i}$ is the simulated yield predicted by the GCM *k,* and for the growing season *i*, and $y_{baseline,i}$ is the baseline yield simulated for the growing season *i*. The box and whiskers plots show the distribution of responses for each growing season. The horizontal line represents the median, the box delimits the 25th and 75th percentiles, and the whiskers the 10th and 90th percentile, respectively.

From the start of simulation to the day of sowing (SP), from sowing to anthesis (PA), and from anthesis to maturity (AM) the delta (Δ) changes of rainfall and days of daily maximum temperature > 34 °C (*Tmax > 34°C)* was calculated. This temperature threshold was chosen because it was linked to heat stress and yield reductions due to acceleration in senescence rates (Asseng et al., 2011). It was calculated as follows:

$$\Delta = RCP_{var,i} - Baseline_{var,i} \quad (4)$$

where $RCP_{var,i}$ is the variable under each of the scenario and each sowing time (*i*), and $Baseline_{var,i}$ is the variable under baseline conditions and each sowing time (*i*).

The extractable water content values for each location, each sowing and each climate scenario were calculated as Delta respect to the start of the simulation date.

$$\Delta Extractable\ water = ewc_d - ewc_s \quad (5)$$

ewc_d represents the extractable soil water content at either Planting (P), anthesis (A), Maturity (M) and ewc_s is the extractable soil water content at the start of simulation (S).

To calculate the magnitude of yield variability coming from the inter-annual baseline climate variability, future climatic variability, the sowing date and the three climate projections (Dry, Mid, Wet) the approach described in Asseng et al. (2013) was considered. For each location and at baseline, the variability across sowing date and within each sowing date (inter-annual variability) was calculated by computing the averages of yield. Then, the standard deviation between years and between locations was computed. For each scenario, the delta yield between baseline and future was calculated. Then the averages and standard deviations between the scenarios and the sowing dates was calculated. Once all the average and standard deviations were calculated the Coefficient of Variation was calculated for the inter-annual variability, the Sowing-Baseline, Sowing-Future, and Scenarios. All the figures were drawn using the library GGPLOT2 from the statistical package R (Wickham, 2016).

3. Results

The calibration of the generic barley cultivar following the information presented on the study of Francia et al. (2011) showed a good agreement between simulated and observed data for both phenology and yield, with d-Index values always above 0.5 (Table 1). For the evaluation of the model, not all the sites had the phenology information, and, when available they were used. Overall, phenology was well simulated, with a RMSE of 6 and 10 days for anthesis and maturity, respectively (Table 1). The observed yield values for the calibration and evaluation dataset are reported in Supplemental Material (Table A4). Overall, the yields under irrigated conditions did not vary too much, while under rainfed conditions observed yields ranged between 70 kg DM ha^{-1} in Jordan to 5400 kg DM ha^{-1} in Syria (Table A4). The simulated yields for the evaluation dataset showed that in some location's yields were under-estimated. For example, in Jordan (JORB) yields were 70 kg DM ha^{-1} for the observed and 1439 kg DM ha^{-1} for the simulated one (Tab. A4).

The reconstructed long-term weather series using AgMERRA, when compared with the observed growing season data showed good agreement between the data (Supplemental Material Figs. 1–4). For solar radiation the RMSE was 3.7 MJ d^{-1} m^{-2} (Fig. A1), while for daily maximum and minimum temperature it was 2.8 and 3.5 °C, respectively (Figs. A2 and A3). Growing season rainfall was compared by plotting the bar plots of the frequency of rainfall at every 2 mm intervals and a good agreement between the observed and the AgMERRA data was found (Fig. A4).

The list of the 40 GCMs for the RCP4.5 Mid of the Century is shown in Supplemental Table 1. At RCP4.5 all the GCM projected an average mean growing season temperature increase between 7 and 18% (Table 2). On the other hand, the differences in changes in growing season rainfall were rather large among GCMs. The overall range of coefficient of variations of the growing season rainfall ranged between 108 and 380%. The three GCM at each location were named as "Dry", "Mid", and "Wet" and had an overall growing season rainfall change of -19%, 0.2%, and +18%, respectively (Table 2).

The mean growing season temperature was higher for GCMs with respect to the baseline and among the 3 GCMs it was higher for the drier scenario; it increased for later sowing dates at all location (Fig. A5). There was a degree of variability among locations, with Jordan and Turkey showing the greatest variability of mean temperature, especially for the Dry scenario (Fig. A5). Growing season rainfall showed higher variability than temperature even for the baseline climate data. Some locations (e.g. Jordan-Ramtha, Spain and Turkey) had little variability of growing season rainfall for any sowing dates, while others (e.g. Italy Fiorenzuola) where rather variable (Fig. A6).

Simulated impacts of climate change on grain yield showed an overall mean yield change of -27%, +4%, +8%, for the Dry, Mid, and Wet scenarios, respectively (Fig. 2). There was a strong location effect with positive mean changes for all the scenarios at Italy-Fiorenzuola, and with strong negative effects for all the scenarios at Jordan-Rabba (Fig. 2). The negative impact of the Dry scenario was consistently high at Jordan-Ramtha with -65% simulated yield. However, at the same location, the Wet scenario showed an overall increase of 25% of grain yield (Fig. 2). The results of the simulations under the Wet scenario showed a higher variability of yield response at each sowing date. The impact of sowing dates on simulated yield depends on the scenario and location considered. Under the Dry scenario late sowings caused an overall 44% yield reduction with respect to early sowing, consistently reducing yield at each location (Fig. 2). On the other hand, under the Wet scenario there was an overall 50% increase of simulated yield with later sowing dates. There is less consistency among locations; for example, at Jordan-Rabba and Spain there was no yield benefit from later sowing (Fig. 2).

The impact of heat and drought on simulated grain yield is shown in

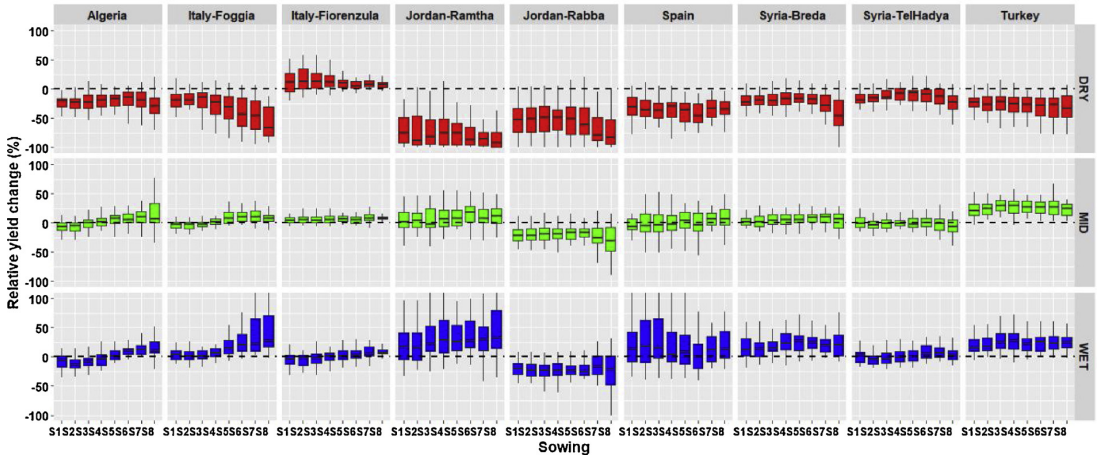

Fig. 2. Simulated relative grain yield change for the eight sowing dates and for the "Dry" (red boxplots), "Mid" (green boxplots), and "Wet" (blue boxplots) scenarios. For each boxplot, the end of the vertical line represents, from top to the bottom, the 10th percentile and the 90th percentile. The horizontal line of the box, from the top to the bottom represents the 25th, median, and 75th percentile, respectively (For interpretation of the references to colour in this figure legend, the reader is referred to the web version of this article).

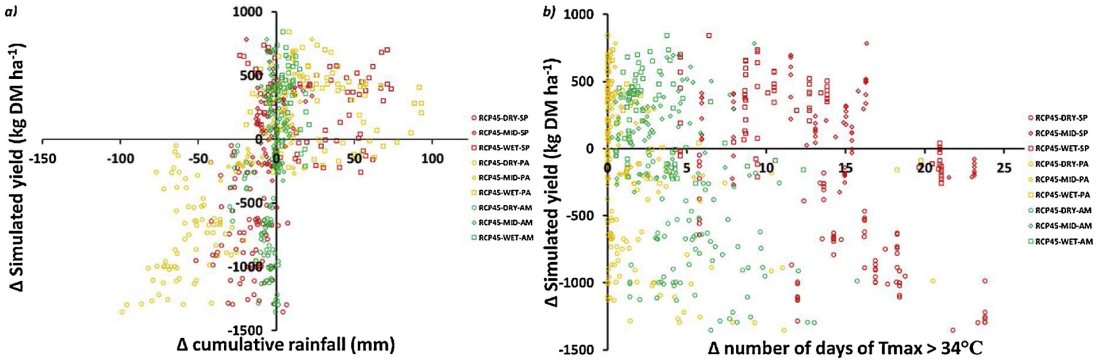

Fig. 3. Relationship between Δ simulated grain yield and (***a***) Δ cumulative rainfall and (***b***) number of days of *Tmax* > 34 °C. The three different GCMs were reported in symbols' shape, with circle being the "Dry", diamond being the "Mid", and square being the "Wet". The different stages were reported with different colour-code, start of simulation to sowing (SP, red), sowing to anthesis (PA, yellow), and anthesis to maturity (AM, green). (For interpretation of the references to colour in this figure legend, the reader is referred to the web version of this article).

Fig. 3. The negative values of the Δ indicated that the values under baseline conditions were higher than the ones under the given scenario and the given crop stage. The amount of rainfall that fell before sowing (defined as the period from a generic harvest time and the sowing date and referred to as fallow rainfall) was -22, 2, and 25 mm under the Dry, Mid, and Wet scenarios, respectively (Fig. 3a, red symbols). There was little response of yield changes as changes in fallow rainfall, except with the Wet scenario where at given increased of Δrain corresponded increases of Δyield (Fig. 3a; red squares). Between sowing to anthesis (PA, yellow symbols) the simulated yield under the dry scenario showed negative responses to changes in rainfall during the vegetative stage. There was a change from -13 to −100 mm of rainfall during this stage across the locations and sowing dates, and this showed a decline in yield between -49 to -1351 kg DM ha^{-1} (Fig. 3a). From anthesis to maturity (AM; green symbols) there were little changes in rainfall which might not be cause of the changes in simulated yields (Fig. 3a). The Δ number of days of *Tmax* > 34 °C was higher for the Dry scenarios at SP, PA, and AM (Fig. 3b). The Δyield under the Wet scenario ranged between -259 to 845 kg DM ha^{-1} (Fig. 3b). The number of days of *Tmax* > 34 °C was between 6 to 24 days, and 0 and 15 days, at SP and PA across the GCMs, respectively (Fig. 3b). The main difference was between AM when the number of days of *Tmax* > 34 °C diverged between the Dry and Wet scenarios, with the former showing on average 5 additional days of *Tmax* > 34 °C (Fig. 3b).

At reproductive stage, the number of days of *Tmax* > 34 °C showed a strong location effect and degrees of variability for each sowing date (Fig. 4). When simulations were run under baseline weather, the average number of days of *Tmax* > 34 °C ranged across locations between 0 and 20. Later sowing dates showed the highest number of days of *Tmax* > 34 °C (Fig. 4). The inter-annual variability, represented by the individual boxplot, did not differ too much within and across locations. One location, Italy Fiorenzuola, did not have any day of *Tmax* > 34 °C, while a location like Syria-Breda showed the highest number of days of *Tmax* > 34 °C ranging from an average 10 at S1 to 20 at S8. Under the Dry scenario, the number of days of *Tmax* > 34 °C increased at all the locations, with two location showing evident changes with respect to the others. At Italy-Fiorenzuola, the number of days *Tmax* > 34 °C changed from 0 to an average of 2.5, and at Jordan-Rabba they increased from an average of 5.5 to 18 days (Fig. 4). At the latter location, such increase is more evident for later planting time; while in Syria-Breda where at S8 there was an increase of 10 days with respect to the baseline (Fig. 4). The number of days of *Tmax* > 34 °C

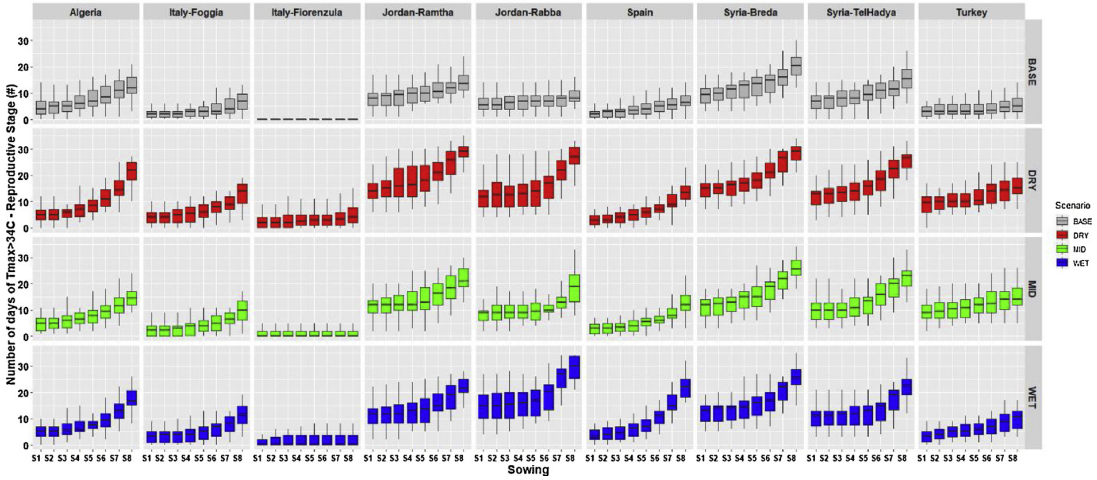

Fig. 4. Number of days of *Tmax* > 34 °C at the reproductive stage for the eight sowing dates and for the Baseline (grey boxplots), "Dry" (red boxplots), "Mid" (green boxplots), and "Wet" (blue boxplots) scenarios. For each boxplot, the end of the vertical line represents, from top to the bottom, the 10th percentile and the 90th percentile. The horizontal line of the box, from the top to the bottom represents the 25th, median, and 75th percentile, respectively (For interpretation of the references to colour in this figure legend, the reader is referred to the web version of this article).

Table 2
List of the three Global Circulation Models (GCMs) selected at each location and their simulated changes of growing season mean temperature and rainfall respect to the baseline.

ID	GCM	Site ID	Growing season rainfall changes *(%)*	Growing season temperature changes *(%)*
DRY	MIROC4H	Algeria	−13.63	17.12
DRY	INMCM4	Italy-Foggia	−18.81	7.61
DRY	INMCM4	Italy-Fiorenzuola	−16.41	11.60
DRY	MIROC4H	Jordan-Ramtha	−23.94	14.09
DRY	MIROC4H	Jordan-Rabba	−31.72	12.21
DRY	GFDL-ESM2M	Spain	−15.22	10.65
DRY	MIROC4H	Syria-Breda	−14.66	13.60
DRY	MIROC4H	Syria-Tel Hadya	−14.33	13.46
DRY	GFDL-ESM2G	Turkey	−20.82	18.36
MID	HADCM3	Algeria	1.50	8.83
MID	BBC-CSM1-1	Italy-Foggia	1.14	9.09
MID	CANESM2	Italy-Fiorenzuola	0.24	12.39
MID	BBC-CSM1-1	Jordan-Ramtha	−0.12	10.01
MID	ACESS-1.3	Jordan-Rabba	0.28	7.63
MID	NORESM1-M	Spain	0.45	11.37
MID	GFDL-ESM2M	Syria-Breda	−2.47	8.79
MID	NORESM1-ME	Syria-Tel Hadya	0.93	10.07
MID	GFDL-ESM2M	Turkey	0.24	11.59
WET	BBC-CSM1-1	Algeria	20.98	9.83
WET	HADCM3	Italy-Foggia	10.82	9.02
WET	CNRM-CM5	Italy-Fiorenzuola	16.56	10.96
WET	MPI-ESM-MR	Jordan-Ramtha	24.27	7.15
WET	FGOALS-G2	Jordan-Rabba	20.10	11.71
WET	MIROC4H	Spain	14.59	17.09
WET	INMCM4	Syria-Breda	23.96	7.02
WET	INMCM4	Syria-Tel Hadya	23.67	6.95
WET	CNRM-CM5	Turkey	5.07	12.78

under the Wet scenario was still high but slightly lower than the Dry one. For example, in Syria-Breda, the number of days *Tmax* > 34 °C at S8 was on average 22, 28, and 25 under the Baseline, Dry, and Wet, respectively (Fig. 4). However, at Jordan-Rabba such variable increased by 15% across all the sowing dates with evident changes at S7 and S8 where the number of days of *Tmax* > 34 °C was 27 and 30, respectively (Fig. 4).

The cumulative rainfall from the start of simulation to planting to anthesis and to maturity is shown in Fig. 5. At Sowing, the cumulative amount increased from the early to the later sowing dates for each location and each scenario. However, the cumulated amount at anthesis did not show such difference. At Jordan-Rabba, there was more rainfall at planting for the later sowing dates across all the different scenarios. At the same location, the cumulative rainfall at anthesis was on average of 347, 232, and 417 mm for the baseline, Dry and Wet scenarios, respectively (Fig. 5). At maturity, there was only an additional 5, 5, and 7 mm of rainfall added under the baseline, Dry, and Wet scenario. On the other hand, in the same country but at different location (Jordan-Ramtha), there was lower cumulated rainfall at anthesis, with 235 mm for the baseline, 175 mm for the Dry scenario, and 291 mm for the Wet scenario (Fig. 5). The inter-annual variability, expressed by the boxes' length, was higher for Italy-Fiorenzuola, Algeria, and Italy-Foggia, but for all the other locations, the inter-annual variability of cumulative rainfall was lower. The number of rainy days was higher for the vegetative stage, but it decreased for later sowing dates (Fig. A7).

The cumulative amount of rainfall that fell between summer and sowing determine the amount of water stored in the soil. Such information is plotted in Fig. 6 and calculated using Eq. (5). The flat lines represent the initial extractable soil water content in summer, when crop simulation was started. The negative values indicated that there was more water at the start of the simulation with respect to a point in time. It does not show the dynamic, but from the simulated daily soil extractable water content key points in time were selected (Fig. S8). The initial conditions of soil water slightly differ among locations due to the information used as initial values from the work of Francia et al. (2011). At sowing, across all the locations and sowing dates there was a range of extractable water of -70 and 174 mm for the baseline, -70 to 159 mm for the Dry scenario, and -72 and 186 mm for the Wet Scenario (Fig. 6). At anthesis, the extractable water content ranged between values of -81 to 126 mm, -75 to 92, and -72 to 125 mm for the baseline, Dry and Wet scenarios, respectively (Fig. 6). In addition, such values decreased further at maturity ranging between -81 to 28 mm for the baseline, -80 to 7 mm for the Dry scenario and -83 to 54 mm for the Wet scenario. At sowing, there was a strong effect of the sowing dates, with the S5 to S8 showing the higher amount of extractable water content (Fig. 6). For Italy-Fiorenzuola, from S3 to S8 the extractable soil water content was higher than the initial one; but, similar patterns were found for Italy-Foggia, and Syria-Tel Hadya. At this latter location, however, the impact of later sowing dates on the extractable soil water content was evident. In fact, at planting date S1 the average extractable soil water was -17 mm with a very narrow inter-annual variability, at anthesis it was 10 mm, with some year having −40 mm and other years reaching 50 mm (Fig. 6). On the other hand, at planting date S8 there was an average of 70 mm with some years showing extractable soil water of 134 mm. However, by anthesis, the average soil water content was -17 mm, and even the year with the high extractable soil water showed a −13 mm of extractable water (Fig. 6). There was a high inter-annual variability at planting for extractable soil water content, it was mirroring the amount of cumulated rainfall (Fig. 5); but it was sowing date- and location-specific.

At Jordan-Rabba, the Wet scenario results showed negative yield changes at each sowing date (Fig. 2). At this specific location there was a high number of days of *Tmax* > 34 °C which were negatively related to simulated yield (Fig. 7a). At anthesis, for the Wet scenarios, there was up to 400 mm of cumulated rainfall, but the simulated yield was only 2200 kg DM ha^{-1} and there was no yield increase beyond 300 mm of rainfall cumulated at anthesis (Fig. 7b). A similar relationship was observed between rain, grain yield and the Δ-extractable soil water content at anthesis (Fig. S9). There was also a linear negative relationship between Δ extractable soil water content at anthesis and number of days of *Tmax* > 34 °C (Fig. 7c). In fact, for the Dry scenario at 26 days of *Tmax* > 34 °C there was the maximum Δ of extractable soil water content of −65 mm (Fig. 7c). The relationship between Δ extractable soil water content at anthesis and cumulative rainfall at

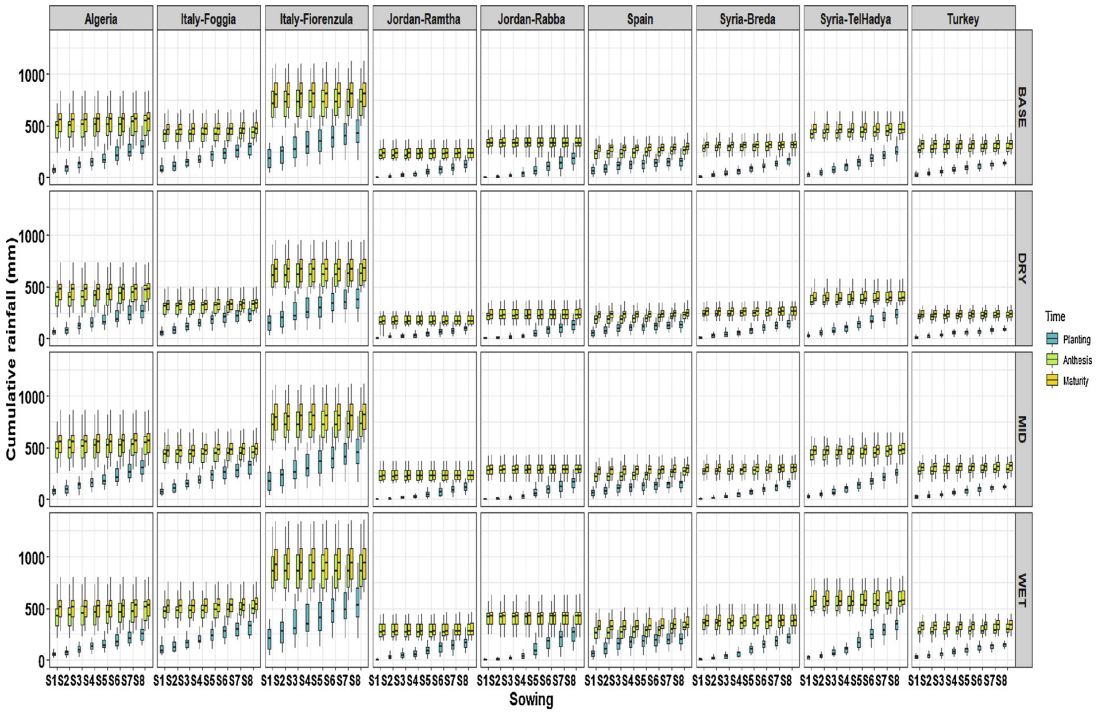

Fig. 5. Cumulative growing season rainfall at sowing (blue box), at anthesis (green box) and at maturity (yellow box) for the baseline, "Dry", "Mid", and "Wet" scenarios. For each boxplot, the end of the vertical line represents, from top to the bottom, the 10th percentile and the 90th percentile. The horizontal line of the box, from the top to the bottom represents the 25th, median, and 75th percentile, respectively (For interpretation of the references to colour in this figure legend, the reader is referred to the web version of this article).

anthesis was linear, with high rainfall corresponding to lower Δ extractable soil water content at anthesis (Fig. 7d).

The variation due to inter-annual weather patterns was the component that carried most of the variability at each of the locations, ranging from 19 to 100% (Fig. 8). The different scenarios also showed higher variability, ranging from 5 to 79% across locations. The variability given by sowing dates under future conditions was lower than the ones under baseline conditions, probably due to the impact of the different scenarios used. Some locations showed higher variability than others, especially Jordan-Ramtha, Jordan-Rabba and Spain, where the inter-annual variability ranged between 77 to 100% (Fig. 8). At those location, the future scenarios also had higher variability with values ranging from 52 to 79%. In Italy-Foggia, the variability due to the scenarios was slightly higher than the inter-annual variability and in Italy-Fiorenzuola, except the inter-annual variability, all the other factors did not show higher values of variability (Fig. 8).

4. Discussion

Different climate projections showed contrasting impacts of simulated barley yield at each location across the Mediterranean environment due to rainfall and temperature changes. At some location (e.g. Italy), the impact of extractable soil water content was more relevant than the heat stress, while in others the number (e.g. Jordan) of days of $Tmax > 34\,^{\circ}C$ caused significant yield decrease. Agronomic adaptations, such as shifting sowing dates minimize the negative impacts of climate change. The inter-annual weather variability impacts barley yield irrespective of the sowing dates and the future projected climate.

The results of the barley model evaluation are in line with the ones reported in other studies where the coefficient of determination for simulated yield was 0.88 (Trnka et al., 2004); Al-Bakri et al. (2010) reported values of RMSE for simulated yields of 586 kg DM ha^{-1}, while values ranging between 292 and 720 kg DM ha^{-1} were reported in Fatemi et al. (2014).

The simulation of barley phenology was also in line with RMSE for heading of 5.6 days reported by Travasso and Magrin (1998). In this study, the RMSE for the simulated yield at evaluation was slightly higher, but this is due by three experiments in Jordan having observed yields of 70, 500, and 800 kg DM ha^{-1}, which caused an overestimation of yield at such locations. The reason for some other lack of fit between observed and simulated data was because at some locations it was observed a severe frost impact (e.g. in Fiorenzuola), while in others, there was a poor canopy vigour leading to lower observed yields. The crop model was set up for running in conditions of good establishment and any damages other than heat and drought are currently not considered. Table A4 showed the reasons why some simulated yields could not reproduce the observed values (frost or poor canopy vigour), but in one case, JORB there were no indications on why 70 kg DM ha^{-1} were observed. Due to the length of time passed from that field experiment there was no record of what really happened. It was decided to keep it for the sake of clarity.

The gap-filling process using the AgMERRA dataset was made only after comparing the observed dataset available with the downloaded data. Overall, the results are in line with the reported outputs from Ruane et al. (2015) indicating the suitability of using the AgMERRA product for the baseline period (1980–2010). Such dataset has been used in numerous studies of climate change impacts as baseline period, allowing meaningful comparisons of climate impacts during the 1980–2010 period (Xie et al., 2018; Asseng et al., 2013, 2015; 2016; Rosenzweig et al., 2014; Elliott et al., 2015). In the current study, some locations (e.g. Turkey) showed an over-estimation of solar radiation by AgMERRA and an under-estimation of minimum and maximum temperature (Figs. A1-A3). On the other hand, locations like Syria-Breda and Jordan-Ramtha showed the opposite behaviour. Such bias could

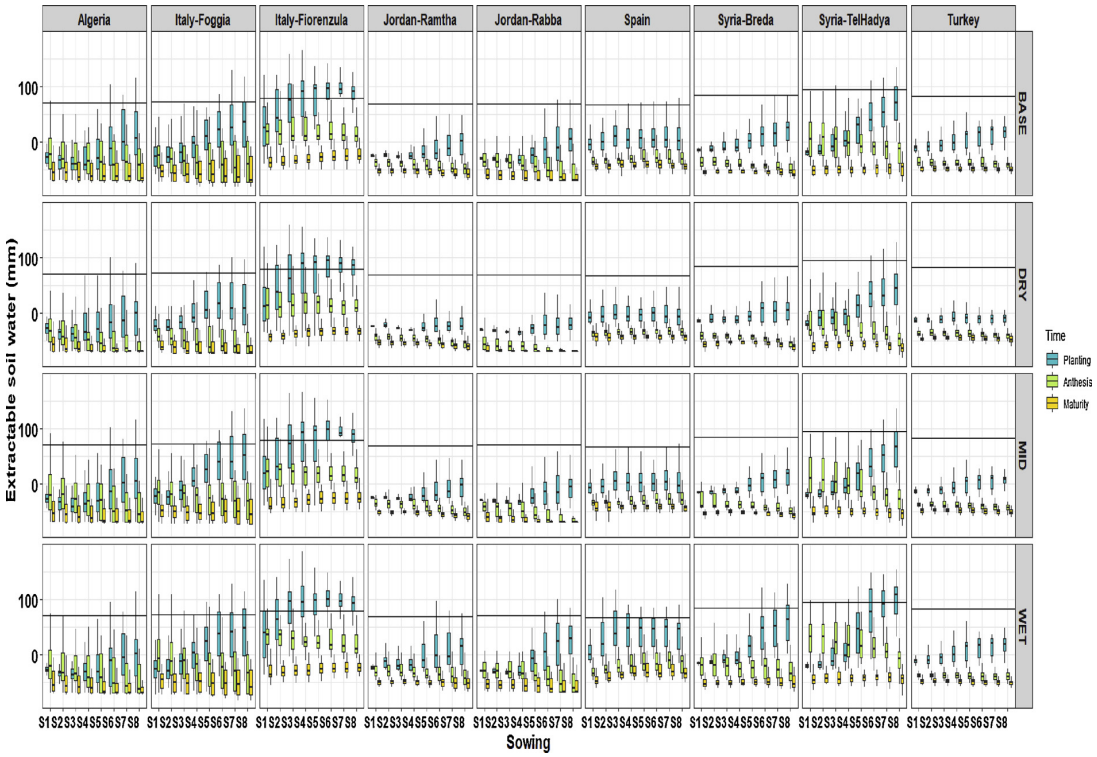

Fig. 6. Extractable soil water content at the start of the simulation (full horizontal line), at sowing (blue box), at anthesis (green box) and at maturity (yellow box) for the baseline, "Dry", "Mid", and "Wet" scenarios. For each boxplot, the end of the vertical line represents, from top to the bottom, the 10th percentile and the 90th percentile. The horizontal line of the box, from the top to the bottom represents the 25th, median, and 75th percentile, respectively (For interpretation of the references to colour in this figure legend, the reader is referred to the web version of this article).

impact the simulated yield because an overestimation of daily temperature means that crops will be subjected to higher than normal temperatures and therefore exacerbate the response to heat stress. However, the over/underestimation of weather variable on the baseline simulation has been quantified to be on average 15% for simulated yield. Taylor et al. (1999) reported that the variation of wheat yields in field experiments is about 13.5%. Therefore, we considered that our bias introduced by the AgMERRA product to be in the range of the observed error.

Reported changes in simulated yield in this study were disaggregated by the type of climate scenario used at a given RCP. Overall, the average climate impact on grain yield across the three scenarios was 9%, in line with the 15% reported results in Al-Bakri et al. (2010) for Jordan and with the mean global reduction of 10% reported in Xie et al. (2018). And, it is also in line with experimental results on other cereal crops (wheat) as reported in field experiments (Ottman et al., 2012; Asseng et al., 2015). The simulation study of Al-Bakri et al. (2010) could be used as benchmark against our simulated results in Jordan. However, their results were obtained by adding incremental changes of either rainfall or temperature. As a result, they could evaluate the sensitivity of rainfall changes at a given temperature level (e.g. keeping temperature constant but varying rainfall). In this study, the dynamic changes of temperature and rainfall were analysed together because they will most likely act as a system. In fact, results of this study showed that under the Dry scenario the mean growing season temperature tends to be slightly higher than the one under the Wet scenarios, which is likely to be caused by more radiation under a Dry scenario than under a cloudy Wet scenario.

There was an interaction between the amount of rainfall, the extractable soil water content and the maximum air temperature as evident in Jordan-Rabba. In that location at higher maximum temperatures there was less extractable soil water and lower yields. However, the impact of the different amount of rainfall and heat differs among locations in the same country. For example, in Jordan the Wet scenarios showed contrasting results at the two locations. Both Rabba and Ramtha had clay soils, with similar plant available water content; at Jordan-Ramtha there was on average 137 mm of available soil water content for the soil depth, while at Jordan-Rabba was 142 mm (Tab. A2). However, Jordan-Rabba had higher number of days of $Tmax > 34$ °C and even if it had a higher extractable soil water content it did not counteract the impact of higher temperatures. The high number of days of $Tmax > 34$ °C caused higher soil water depletion from the plant and therefore lower yields under the wet scenario. In addition, Asseng et al. (2011) concluded that daily maximum temperatures above 34 °C means that leaf senescence rates are accelerated 3-folds, and such higher temperature has also a negative impact of grain filling rates and grain abortion rates (Fischer et al., 1980). Liu et al. (2016) compared simulated and observed data of the impacts of heat stress at anthesis and grain filling stages. They found that for every unit increase of heat degree-days grain yield was reduced by 1.0–1.6%. The CERES-Wheat model used in this study has also been evaluated in many locations across Asia, Europe, and America encompassing a variety of pedo-climatic conditions (Koo and Rivington, 2005; Timsina and Humphreys, 2006). Crop growth is directly related to the amount of soil water/rainfall, solar radiation, and nutrient availability to the crop. These factors are interrelated, because while roots are responsible to uptake water and nutrients the canopy is responsible for capturing solar radiation and CO_2 and then transform these into biomass (Jamieson and Ewert, 1999; Sadras and Angus, 2006). Therefore, the results of this study are an attempt to start considering the whole system together

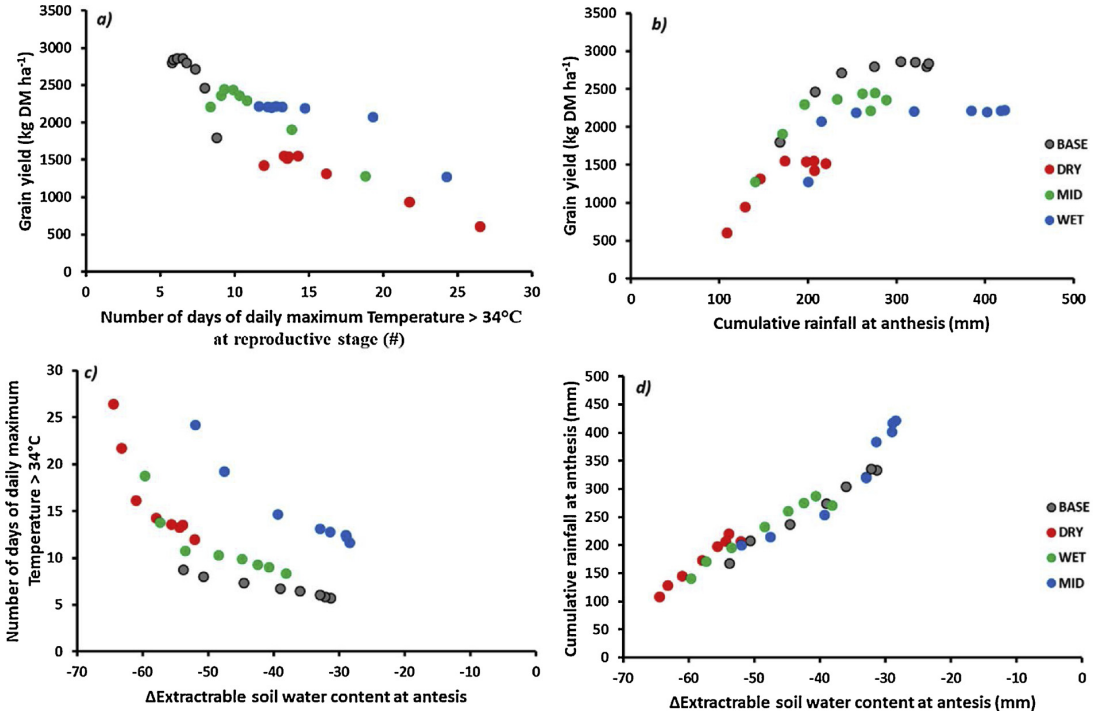

Fig. 7. Relationship between (*a*) number of days of *Tmax* > 34 °C at reproductive stage and simulated grain yield; (*b*) cumulative rainfall at anthesis and grain yield; (*c*) Δextractable soil water content at anthesis and number of days of *Tmax* > 34 °C at reproductive stage; and (*d*) Δextractable soil water content at anthesis and cumulative rainfall at anthesis for the baseline (grey dots), Dry (red dots), Mid (green dots), and Wet (blue dots) scenarios at Jordan-Rabba. (For interpretation of the references to colour in this figure legend, the reader is referred to the web version of this article).

where the impact of temperature is not considered *per-se,* but it is also analysed as function of the location-specific soil characteristics. By running the crop simulation model from the summer prior sowing this study accounted also the water stored prior sowing which in such environments is an important determinant of grain yield as found in other studies (Basso et al., 2010, 2011, 2012; Sadras, 2002; Sadras et al., 2012). The overall amount of stored water in the soil over the winter period would also help to minimize the impact of the inter-annual variability on grain yield under current and future climate projections. This was evident in some locations like Foggia (Italy) were simulated yields responded positively to the Wet scenario and for the late sowing dates. In that location, the number of days of Tmax > 34 °C is similar for the Dry and Wet scenarios but simulated yields were higher for the Wet than the Dry scenario (Fig. 2). Fig. 6 showed that for the Wet scenario Foggia held higher extractable water content for later sowing dates as a result of accumulation of stored water. This means that respect to the earlier sowing dates, later sowing will take advantage of more stored water to help their growth, especially in the earlier phases.

To preserve the soil water content and improving grain yield, farmers will need to adopt different sustainable agronomic practices. On the one hand, the shifting of sowing dates is a viable adaptation option for escaping terminal drought in this environment. Another agronomic practice that was not considered in this study, aimed at increasing soil water content is through the improvement of the soil

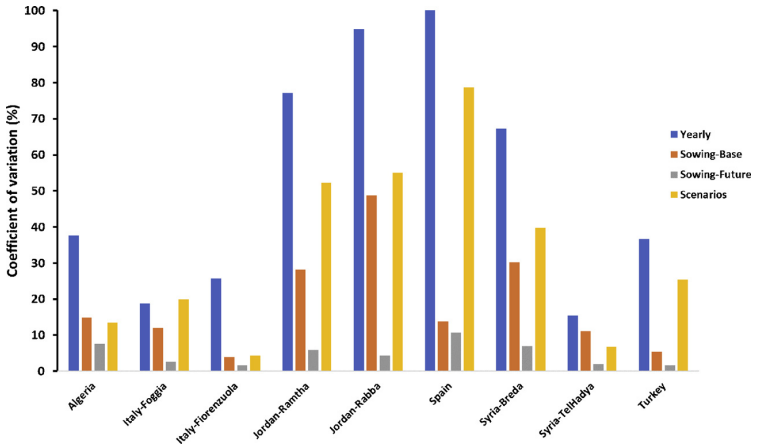

Fig. 8. Coefficient of variation due to the inter-annual variation (Yearly; blue bars), the sowing dates under the baseline conditions (Sowing-Base; orange bars), the sowing dates under future conditions (Sowing-Future; grey bars); and the different scenarios used (Scenarios; yellow bars) (For interpretation of the references to colour in this figure legend, the reader is referred to the web version of this article).

organic carbon (Rawls et al., 2003). Anjum et al. (2011) studying maize (*Zea mays* L.) suggested that, exogenous applications of fulvic acid substantially ameliorated the adversities of drought increasing canopy chlorophyll. These beneficial effects might be tested also on barley when cropped in the Mediterranean basin.

Ceccarelli et al. (2000) suggested that along with agronomy, breeding is an important aspect to take into consideration. Timing and duration of reproductive stages are two important factors affecting breeding strategies. In fact, matching the crop development to the environmental resources is one the greatest challenge for achieving higher yields in new genotypes (Ceccarelli et al., 2000; Mitterbauer et al., 2017). In Mediterranean environments terminal drought is a known problem and results of this study show that it will be exacerbated by climate change. Because of the different nature and intensity of the terminal drought, traits such as root architecture (Richards et al., 2010) or prostrate habit, vigorous seedling growth, good ground cover, early ear emergence, many ears m^{-2} and large grains (Acevedo et al., 1991) may play a different role in different locations.

There are several limitations to this study, the cultivar used is a generic barley variety calibrated in the Mediterranean basin and does not consider genetic differences among cultivars as done in Zheng et al. (2013). Furthermore, it does not consider current and future breeding activities for adaptation that may lead to more resilient barley genotypes. This is particularly relevant for this species, with genotypes locally adapted to a diversity of potential extreme growing conditions. In addition, the model does not use canopy temperatures in the simulations. The canopy temperature can be cooler than the air temperature by several degrees during transpiration due to evaporative cooling (Kumar and Tripathi, 1991) or can be warmer by several degrees in situations where there is no soil water available for transpiration (Fischer et al., 1980). Although important for such kind of studies there is a recent scientific effort to understand the best modelling approach for considering canopy temperature impacts (Webber et al., 2017, 2018).

5. Conclusions

The impact of future climate on barley yield in the Mediterranean is negative. Such impact differs among locations, with some areas being worse off than others are. However, the negative impact of climate change depends on the climate projection considered, as some of the GCMs showed an increase in growing season rainfall. The increase in rainfall does not always translates into higher yields because the number of days of $Tmax > 34\,^{\circ}C$ at reproductive stage offsets such gains. The current sowing window across the Mediterranean basin (Sep-Dec) will still be relevant under future conditions, linking climate forecasts systems with crop simulation models could help to refine the sowing window for each growing season.

Acknowledgments

Prof. A. Suleiman for kindly providing soil information at the locations in Jordan. We also thank the referees for the valuable comments and suggestions that helped to improve the manuscript.

Appendix A. Supplementary data

Supplementary material related to this article can be found, in the online version, at doi:https://doi.org/10.1016/j.eja.2019.03.002.

References

Acevedo, E., Craufurd, P.Q., Austin, R.B., Perez-Marco, P., 1991. Traits associated with high yield in barley in low-rainfall environments. J. Agric. Sci. 116 (1), 23–36.
Al-Bakri, J., Suleiman, A., Abdulla, F., Ayad, J., 2010. Potential impact of climate change on rainfed agriculture of a semi-arid basin in Jordan. Phys. Chem. Earth 35, 125–134.
Anjum, S.A., Wang, L., Farooq, M., Xue, L., Ali, S., 2011. Fulvic acid application improves the maize performance under well-watered and drought conditions. J. Agron. Crop. Sci. 197 (6), 409–417.
Asseng, S., Foster, I., Turner, N.C., 2011. The impact of temperature variability on wheat yields. Glob. Change Biol. 17, 997–1012.
Asseng, S., Ewert, F., Rosenzweig, C., Jone, J.W., Hatfield, J.L., Ruane, A.C., Boote, K.J., Thorburn, P.J., Rotter, R.P., Cammarano, D., Brisson, N., et al., 2013. Uncertainty in simulating wheat yields under climate change. Nat. Clim. Change. https://doi.org/10.1038/nclimate1916.
Asseng, S., Ewert, F., Martre, P., et al., 2015. Rising temperatures reduce global wheat production. Nat. Clim. Change 5, 143–147.
Asseng, S., Cammarano, D., Basso, B., Chung, U., Alderman, P.D., Sonder, K., Reynolds, M., Lobell, D.B., 2016. Hot spots of wheat yield decline with rising temperatures. Glob. Change Biol. https://doi.org/10.1111/gcb.12530.
Basso, B., Cammarano, D., Troccoli, A., Chen, D., Ritchie, J.T., 2010. Long term wheat response to nitrogen in a rainfed Mediterranean environment: field data and simulation analysis. Eur. J. Agron. 33, 132–138.
Basso, B., Ritchie, J.T., Cammarano, D., Sartori, L., 2011. A strategic and tactical management approach to select optimal N fertilizer rates for wheat in a spatially variable field. Eur. J. Agron. 35, 215–222.
Basso, B., Fiorentino, C., Cammarano, D., Cafiero, G., Dardanelli, J., 2012. Analysis of rainfall distribution on spatial and temporal patterns of wheat yield in Mediterranean environment. Eur. J. Agron. 41, 52–65.
Brisson, N., Gate, P., Gouache, D., Charmet, G., Oury, F.X., Huard, F., 2010. Why are wheat yields stagnating in Europe? A comprehensive data analysis for France. Field Crop Res. 119, 201–212.
Cammarano, D., Tian, D., 2018. The effects of projected climate and climate extremes on a winter and summer crop in the southeast USA. Agric. For. Meteorol. 248, 109–118.
Ceccarelli, S., Grando, S., Tutwiler, R., Baha, J., Martini, A., Salahieh, H., Goodchild, A., Micheal, M., 2000. A methodological study on participatory breeding I. Selection phase. Euphytica 111, 91–104.
Ceccarelli, S., Grando, S., Capettini, F., 2011. Barley breeding history, progress, objectives, and technology, near East, North and East Africa and Latin America. In: Ullrich, S.E. (Ed.), Barley: Production, Improvement and Uses. Wiley-Blackwell, Ames (Iowa), USA, pp. 210–220.
Challinor, A.J., Watson, J., Lobell, D.B., Howden, S.M., Smith, D.R., Chhetri, N., 2014. A meta-analysis of crop yield under climate change and adaptation. Nat. Clim. Change 4, 287–291.
Dawson, I.K., Russel, J., Powell, W., Steffenson, B., Thomas, W.T.B., Waugh, R., 2015. Barley: a translational model for adaptation to climate change. New Phytol. https://doi.org/10.1111/nph.13266.
Elliott, J., Muller, C., Deryng, D., Chryssanthacopoulos, J., Boote, K.J., Buchner, M., Foster, I., Glotter, M., et al., 2015. The global gridded crop model intercomparison: data and modeling protocols for phase 1 (v1.0). Geosci. Model. Dev. https://doi.org/10.5194/gmd-8-261-2015.
FAOSTAT, 2018. Food and Agriculture Organization of the United Nations, Viale Delle Terme Di Caracalla, 00153 Rome, Italy. (Accessed November 2018). http://www.fao.org/faostat/en/#home.
Fatemi, Z., Pknejad, F., Amiri, E., Eilkaee, M.N., 2014. Capability of the CERES-Barley model for prediction of barley varieties growth under deficit irrigation. J. Biol. 2, 1–7.
Fischer, R.A., 1980. Influence of water stress on crop yield in semiarid regions. In: Turner, N.C., Kramer, P.J. (Eds.), Adaptation of Plants to Water and High Temperature Stress. Wiley, New York, pp. 323–339.
Francia, E., Tondelli, A., Rizza, F., Badeck, F.W., et al., 2011. Determinats of bazrely grain yield in a wide range of Mediterranean environments. Field Crop Res. 120, 169–178.
Food barley: importance, uses and local knowledge. Grando, S., Gormez Macpherson, H. (Eds.), Proceedings of the International Workshop on Food Barley Improvement x +156 pp.
Hoogenboom, G., Jones, J.W., Wilkens, P.W., Porter, C.H., et al., 2010. Decision Support System for Agrotechnology Transfer (DSSAT), Version 4.5 (CD-ROM). University of Hawaii, Honolulu, HI.
Huntingford, C., Hugo Lambert, F., Gash, J.H.C., Taylor, C.M., Challinor, A.J., 2005. Aspects of climate change prediction relevant to crop productivity. Philos. Trans. R. Soc. B: Biol. Sci. 360, 1999–2009.
Jamieson, P.D., Ewert, F., 1999. The role of roots in controlling soil water extraction during drought: an analysis by simulation. Field Crop Res. 60, 267–280.
Jones, J.W., Hoogenboom, G., Porter, C.H., Boote, K.J., et al., 2003. The DSSAT cropping system model. Eur. J. Agron. 18, 235–265.
Kobza, J., Edwards, G.E., 1987. Influences of leaf temperature on photosynthetic carbon metabolism in wheat. Plant Physiol. 83, 69–74.
Koo, J., Rivington, M., 2005. Report on the Meta-analysis of Crop Modelling for Climate Change and Food Security Survey Climate Change. Agriculture and Food Security (CCAFS), Challenge Program, Denmark.
Kumar, A., Tripathi, R.P., 1991. Relationships between leaf water potential, canopy temperature and transpiration in irrigated and non-irrigated wheat. J. Agron. Crop. Sci. 166, 19–23.
Liu, B., Asseng, S., Muller, C., Ewert, F., Elliot, J., et al., 2016. Similar estimates of temperature impacts on global wheat yield by three independent methods. Nat. Clim. Change. https://doi.org/10.1038/nclimate3115.
Lobell, D.B., Burke, M.B., Tebaldi, C., Mastrandrea, M.D., Falcon, W.P., Naylor, R.L., 2008. Prioritizing climate change adaptation needs for food security in 2030. Science 319, 607–610.
Martre, P., He, J., Le Gouis, J., Semenov, M.A., 2015. In silico system analysis of physiological traits determining grain yield and protein concentration for wheat as influenced by climate and crop management. J. Exp. Bot. 66, 3581–3598.
Mitterbauer, E., Enders, M., Bender, J., Erbs, M., Habekuß, A., Kilian, B., Ordon, F.,

Weigel, H.-J., 2017. Growth response of 98 barley (*Hordeum vulgare* L.) genotypes to elevated CO_2 and identification of related quantitative trait loci using genome-wide association studies. Plant Breed. https://doi.org/10.1111/pbr.12501.
O'Leary, G.J., Christy, B., Nuttal, J., Huth, N., Cammarano, D., et al., 2015. Response of wheat growth, grain yield and water use to elevated CO_2 under a Free-Air CO_2 Enrichment (FACE) experiment and modelling in a semi-arid environment. Glob. Change Biol. 21, 2670–2686.
Ottman, M.J., Kimball, B.A., White, J.W., Wall, G.W., 2012. Wheat growth response to increased temperature from varied planting dates and supplemental infrared heating. Agron. J. 104, 7–16.
Passioura, J., 2006. Increasing crop productivity when water is scarce—from breeding to field management. Agric. Water Manag. 80, 176–196.
Porter, J.R., Xie, L., Challinor, A.J., Cochrane, K., Howden, M., Iqbal, M.M., Lobell, D.B., Travasso, M.I., 2014. Chapter 7. Food security and food production systems. Climate Change 2014: Impacts, Adaptation and Vulnerability. Working Group II Contribution to the IPCC 5th Assessment Report, Geneva, Switzerland.
Rawls, W.J., Pachepsky, Y.A., Ritchie, J.C., Sobecki, T.M., Bloodworth, H., 2003. Effect of soil organic carbon on soil water retention. Geoderma 116 (1-2), 61–76.
Richards, R.A., Rebetzke, G.J., Watt, M., Condon, A.G., Spelmeyer, W., Dolferus, R., 2010. Breeding for improved water productivity in temperate cereals: phenotyping, quantitative trait loci, markers and the selection environment. Funct. Plant Biol. 37, 85–97.
Rosenzweig, C., et al., 2014. Assessing agricultural risks of climate change in the 21st century in a global gridded crop model intercomparison. Proc. Natl. Acad. Sci. U. S. A. 111, 3268–3273.
Rosenzweig, C., Hillel, D. (Eds.), 2015. Handbook of Climate Change and Agroecosystems: The Agricultural Model Intercomparison and Improvement Project (AgMIP) Integrated Crop and Economic Assessments. ICP Series on Climate Change Impacts, Adaptation, and Mitigation, vol. 3 Imperial College Press. https://doi.org/10.1142/p970.
Rötter, R.P., Palosuo, T., Kersebaum, K.C., Angulo, C., Bindi, M., et al., 2012. Simulation of spring barley yield in different climatic zones of Northern and Central Europe: a comparison of nine crop models. Field Crop Res. 133, 23–26.
Ruane, A.C., McDermid, S.P., 2017. Selection of a representative subset of global climate models that captures the profile of regional changes for integrated climate impacts assessment. Earth Perspect. https://doi.org/10.1186/s40322-017-0036-4.
Ruane, A.C., Goldberg, R., Chryssanthacopoulos, J., 2015. Climate forcing datasets for agricultural modeling: merged products for gap-filling and historical climate series estimation. Agric. For. Meteorol. 200, 233–248.
Sadras, V.O., 2002. Interaction between rainfall and nitrogen fertilization of wheat in environments prone to terminal drought: economic and environmental risks analysis. Field Crop Res. 77, 201–215.
Sadras, V.O., Angus, J.F., 2006. Benchmarking water-use efficiency of rainfed wheat in dry environments. Aust. J. Agric. Res. 57, 847–856.
Sadras, V.O., Lawson, C., Hooper, P., McDonald, G., 2012. Contribution of summer rainfall and nitrogen to the yield and water use efficiency of wheat in Mediterranean-type environments of South Australia. Eur. J. Agron. 36, 41–54.
Saseendran, S.A., Ahuja, L.R., Timlin, D., Stockle, C.O., Boote, K.J., Hoogenboom, G., 2008. Current water deficit stress simulations in selected agricultural system models. In: Response of Crops to Limited Water: Understanding and Modeling Water Stress Effects on Plant Growth. In: Ahuja, L.R., Reddy, V.R., Saseendran, S.A., Qiang, Y. (Eds.), Advances in Agricultural Systems Modeling 1. American Society of Agronomy, Inc., WI, USA.
Semenov, M.A., Stratonovitch, P., Alghabari, F., Gooding, M.J., 2014. Adapting wheat in Europe for climate change. J. Cereal Sci. 59, 245–256.
Senapati, N., Stratonovitch, P., Paul, M.J., Semenov, M.A., 2018. Drought tolerance during reproductive development is important for increasing wheat yield potential under climate change in Europe. J. Exp. Bot. https://doi.org/10.1093/jxb/ery226.
Tao, F., Rotter, R.P., Palosuo, T., Diaz-Ambrona, C.G.H., Ines Mingues, M., et al., 2018. Contribution of crop model structure, parameters and climate projections to uncertainties in climate change impact assessments. Glob. Change Biol. https://doi.org/10.1111/gcb.14019.
Taylor, S.L., Payton, M.E., Raun, W.R., 1999. Relationship between mean yield, coefficient of variation, mean square error, and plot size in wheat field experiments. Commun. Soil Sci. Plant Anal. 30, 1439–1447.
Taylor, K.E., Stouffer, R.J., Meehl, G.A., 2012. An Overview of CMIP5 and the experiment design. Bull. Am. Meteorol. Soc. 93, 485–498.
Timsina, J., Humphreys, E., 2006. Performance of CERES-rice and CERES-wheat models in rice-wheat systems: a review. Agric. Syst. 90, 5–31.
Travasso, M.I., Magrin, G.O., 1998. Utility of CERES-Barely under Argentine conditions. Field Crop Res. 57, 329–333.
Trnka, M., Dubrovsky, M., Zalud, Z., 2004. Climate change impacts and adaptation strategies in spring barley production in the Czech Republic. Clim. Change 64, 227–255.
Webber, H., Martre, P., Asseng, S., Kimball, B., White, J., Ottman, M., et al., 2017. Canopy temperature for simulation of heat stress in irrigated wheat in a semi-arid environment: a multi-model comparison. Field Crop Res. 202, 21–35.
Webber, H., White, J.W., Kimball, B.A., Ewert, F., Asseng, S., Rezaei, E.E., et al., 2018. Canopy temperature for simulation of heat stress in irrigated wheat in a semi-arid environment: a multi-model comparison. Field Crop Res. 216, 75–88.
Wickham, H., 2016. ggplot2: Elegant Graphics for Data Analysis. Springer-Verlag, New York 2016.
Wilmott, C.J., 1982. Some comments on the evaluation of model performance. Bull. Am. Meteorol. Soc. 63, 1309–1313.
Xie, W., Xiong, W., Pan, J., Ali, T., Cui, Q., Guan, D., Meng, J., Mueller, N.D., Lin, E., Davis, S.J., 2018. Decreases in global beer supply due to extreme drought and heat. Nat. Plants. https://doi.org/10.1038/s41477-018-0263-1.
Yin, C., Li, Y., Urich, P., 2013. SimCLIM 2013 Data Manual. available at. CLIMsystems Ltd, New Zealand. www.climsystems.com.
Zheng, B., Biddulph, B., Li, D., Kuchel, H., Chapman, S., 2013. Quantification of the effects of VRN1 and Ppd-D1 to predict spring wheat (Triticum aestivum) heading time across diverse environments. J. Exp. Bot. https://doi.org/10.1093/jxb/ert209.